Direct Extraction of a Distributed Nonlinear FET Model from Pulsed *I–V*/Pulsed *S*-Parameter Measurements

B. Mallet-Guy, Z. Ouarch, M. Prigent, R. Quéré, and J. Obregon

***Abstract*—In this letter, a method for the direct extraction of a field-effect transistor (FET) distributed model is presented. This technique makes use of both pulsed I–V and pulsed S-parameter measurements. Results given are very efficient, especially in terms of time computation and uniqueness. Using this method, the distributed model provides a reliable mean of describing the FET's distributive nature.**

I. Introduction

THE CLASSICAL field-effect transistor (FET) model, based on a simple π topology, is not able to reproduce with accuracy the FET's behavior, such as power saturation at high frequencies, intermodulation, and nonlinear noise behavior. Thus, it is necessary to take into account the channel-distributed nature under the gate. In this way, a FET nonlinear equivalent circuit, including an internal node and distributed along the gate length, was presented in [1]. Although not including the questionable charging resistor Ri [2, p. 111], thanks to its internal node, the distributed model reproduces the nonquasistatic behavior of the transistor. It has already shown significant improvement of the accuracy of the power saturation simulation at high frequency [1].

To be useful, the model must be easily and quickly extracted from measurement data. In this letter, we present an analytical method to determine the intrinsic elements. The conductances and transconductances are directly calculated from pulsed *I–V* measurements. Then the capacitors are analytically determined from *S*-parameter measurements.

II. Direct Extraction of the FET Distributed Model

Our topology [3] considers the region under the gate like an active transmission line [4], [5]. Each cell of this active line is constituted by a nonlinear voltage-controlled current source (VCCS): I1 and I2. The two cells topology is the simplest distributed one that gives a realistic description of the channel-distributive nature and allows a direct extraction. The distributed gate current is modeled with diodes (Id_1, Id_2, and Id_3) in parallel with each of the three capacitors of the transmission line. The complete description and the way to extract the nonlinear current sources have already been described in [1]. The linearized model of the nonlinear equivalent circuit is shown in Fig. 1.

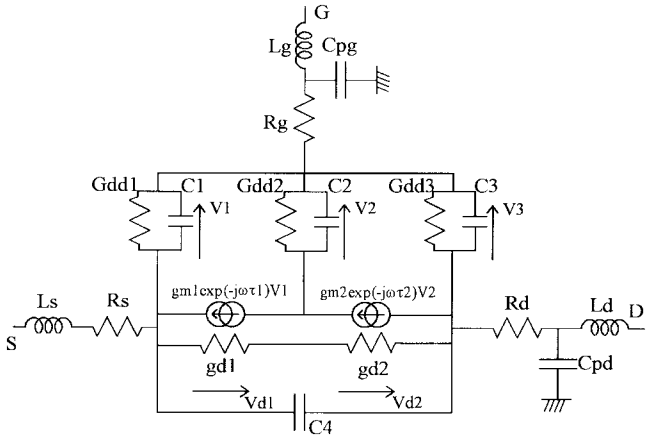

Fig. 1. Schematic of the small-signal distributed model.

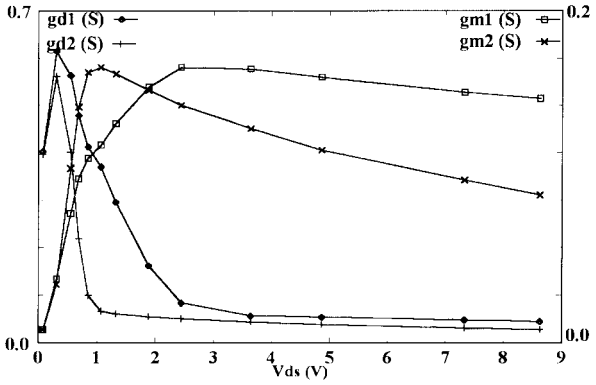

Fig. 2. Transconductances and output conductances variations with V_{ds} for $V_{gs} = -1$ V.

The extrinsic elements are extracted from cold S-parameter measurements. gd_1, gm_1, gd_2, gm_2 are the conductances and transconductances of, respectively, I_1 and I_2. Gdd1, Gdd2, and Gdd3 are the conductances of each diode.

Manuscript received October 9, 1997.
The authors are with I.R.C.O.M., C.N.R.S., 19100 Brive, France.
Publisher Item Identifier S 1051-8207(98)01465-2.

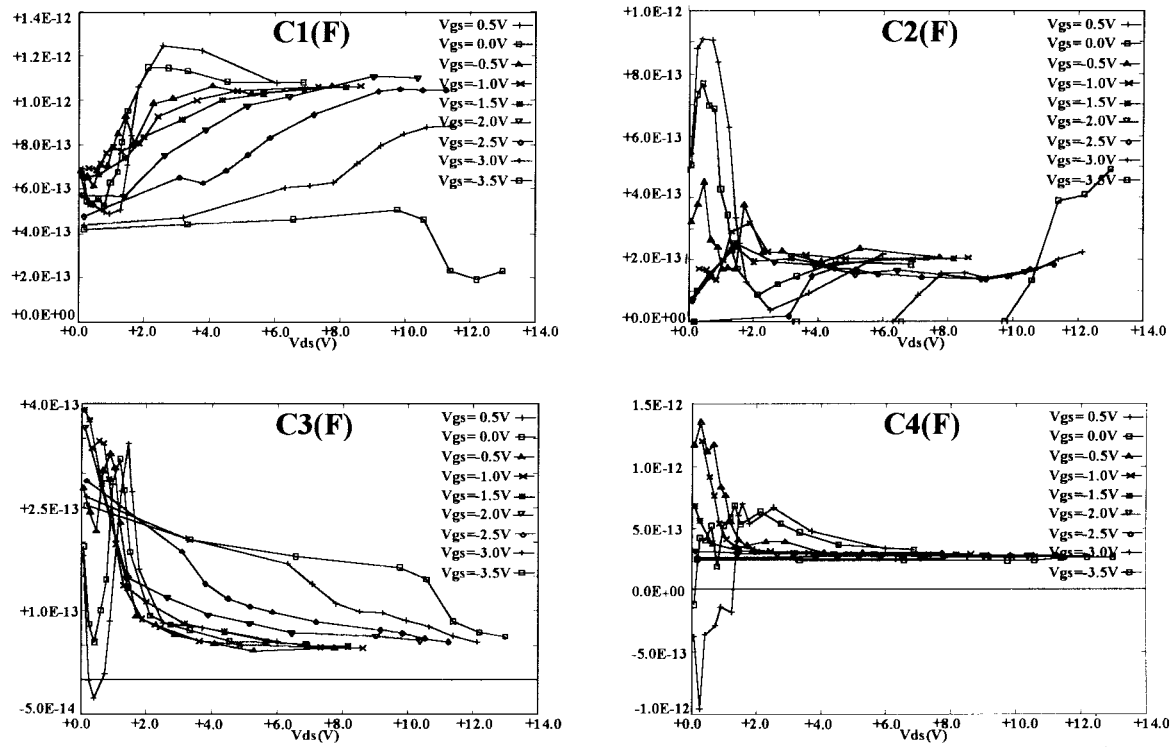

Fig. 3. Extraction of the four capacitors $C_1, C_2, C_3,$ and C_4.

The intrinsic Y parameter expressions are

$$Y_{11} = j\omega C_1 + j\omega C_3 + j\omega C_2 \frac{gd_1 + gd_2 + gm_1 e^{j\omega\tau_1}}{gd_1 + gd_2 + gm_2 e^{j\omega\tau_2} + j\omega C_2}$$

$$Y_{12} = -j\omega C_3 - j\omega C_2 \frac{gd_2}{gd_1 + gd_2 + gm_2 e^{j\omega\tau_2} + j\omega C_2}$$

$$Y_{21} = -j\omega C_3 + \frac{gd_1 gm_2 e^{j\omega\tau_2} + gm_1 e^{j\omega\tau_1}(gm_2 e^{j\omega\tau_2} + gd_2) - j\omega C_2 gd_2}{gd_1 + gd_2 + gm_2 e^{j\omega\tau_2} + j\omega C_2}$$

$$Y_{22} = j\omega C_3 + j\omega C_4 + \frac{gd_2(gd_1 + j\omega C_2)}{gd_1 + gd_2 + gm_2 e^{j\omega\tau_2} + j\omega C_2}.$$

In order to extract the intrinsic elements, we present a method which makes use of both pulsed *I–V* and pulsed *S*-parameter measurements. First of all, $gd_1, gd_2, gm_1,$ and gm_2 are directly determined for all bias points from the derivatives of the model extracted from pulsed *I–V* measurements. This model is obtained by assuming the same nonlinear description of the two cells current sources. Differences between transconductances (Gm_1 and Gm_2) and output conductances (gd_1 and gd_2) arise only from the different biasing of the two cells:

$$gd_1 = \left.\frac{\partial I_1}{\partial V_{d1}}\right|_{V_1}, \quad gm_1 = \left.\frac{\partial I_1}{\partial V_1}\right|_{V_{d1}},$$

$$gd_2 = \left.\frac{\partial I_2}{\partial V_{d2}}\right|_{V_2}, \quad gm_2 = \left.\frac{\partial I_2}{\partial V_2}\right|_{V_{d2}}.$$

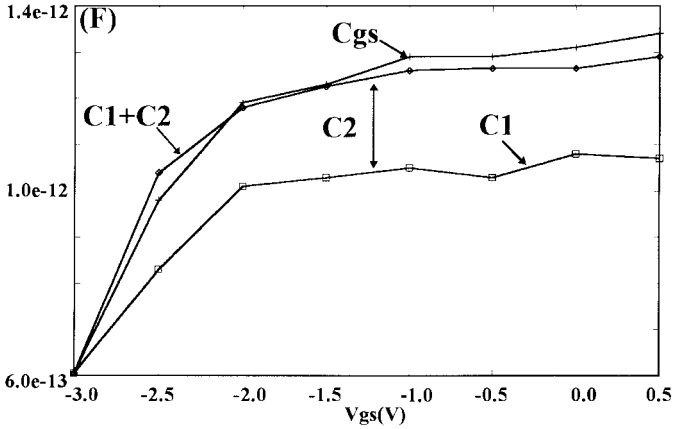

Fig. 4. Variation with V_{gs} for $V_{ds} = 9.8$ V of $C_1 + C_2$ and C_{gs}.

Secondly, for the same bias points and for all the frequencies, $C_1, C_2, C_3,$ and C_4 are analytically calculated from the deembeded Y-parameters and the four conductances and transconductances, using following equations:

$$C_2 = \frac{gm_{2i}(\mathrm{Re}\, Y_{12} + \mathrm{Re}\, Y_{22})\omega + \sqrt{\Delta}}{2\omega^2(\mathrm{Re}\, Y_{12} + \mathrm{Re}\, Y_{22})}$$

$$C_3 = -\frac{1}{\omega}\left[\mathrm{Im}\, Y_{12} + \frac{\omega C_2 gd_2 E_2}{D}\right]$$

$$C_1 = \frac{1}{\omega}\left[\mathrm{Im}\, Y_{11} - \omega C_3 - \frac{\omega C_2}{D}(E_1 E_2 + gm_{1i}(gm_{2i}\omega C_2))\right]$$

$$C_4 = \frac{1}{\omega}\left[\mathrm{Im}\, Y_{22} - \omega C_3 - \frac{1}{D}(\omega C_2 gd_2 E_2 - gd_1 gd_2 - gm_{2i})\right]$$

$R_g = 0.4\ \Omega$	$R_d = 0.8\ \Omega$	$R_s = 0.8\ \Omega$	$L_g = 265$ pH
$L_d = 245$ pH	$L_s = 9$ pH	$C_{pg} = 45$ fF	$C_{pd} = 30$ fF

with

$$E_1 = gd_1 + gd_2 + gm_{1r} \quad E_2 = gd_1 + gd_2 + gm_{2r}$$
$$gm_{xr} = gm_1 \cos(\omega\tau_x) \quad gm_{xi} = gm_1 \sin(\omega\tau_x) \quad (x = 1, 2)$$
$$\Delta = gm_{2i}^2(\mathrm{Re}\, Y_{12} + \mathrm{Re}\, Y_{22})^2\omega^2 - 4\omega^2(\mathrm{Re}\, Y_{12} + \mathrm{Re}\, Y_{22})gd_1\, \mathrm{Re}\, Y_{12}E_2$$
$$D = (gd_1 + gd_2 + gm_{2r})^2 + (\omega C_2 - gm_{2i})^2.$$

Previous extractions and optimizations have already shown that τ_1 may be put equal to zero and τ_2 equal to the τ of the classical model [1]. It is very important to notice that this extraction is reliable only with a pulsed measurements setup [5]. In fact, under such conditions, thermal and trap effects are controlled and thus consistency between $I - V$ and radio frequency (RF) extracted derivatives is ensured.

III. Results

To illustrate the above method we present the extraction results from a 0.5 * 1200 μm^2 transistor. The device was mounted on a chip carrier and connected to access lines with bounding wires. It was biased in a class B mode and the model was extracted from 2 to 18 GHz. Large-signal model validations have been already presented in [1], showing very good agreements between nonlinear simulations and pulsed I–V, pulsed S-parameter, and active load-pull measurements. The values of the eight extrinsic elements are shown at the top of the page.

The results of the direct extraction are presented Figs. 2 and 3. Note that although I_1 and I_2 provide the same current, the variations of gd_1 and gd_2, gm_1, and gm_2 are different. As shown, C_1 and C_3 have, respectively, the same behavior than C_{gs} and C_{gd} (classical model). C_4 is identical to C_{ds}. Fig. 3 shows that in the nonlinear model, C_2, C_3, and C_4 can be taken as constant, especially in the saturated region. For sake of simplicity, only the dependence of C_1 with V_1 is taken into account, so there is no difficulty arising from possible charge nonconservation in the nonlinear model. Fig. 4 represents the variation with V_{gs} for $V_{ds} = 9.8$ V of $C_1 + C_2$ and C_{gs}. This figure is very interesting because it demonstrates that $C_1 + C_2 \approx C_{gs}$. This is explained by the fact that C_{gs} (ohmic region) is distributed into C_1 and C_2. In the same way, C_{gd} (saturated region) is also distributed into C2 and C3. This means that the capacitance of the depleted region is really distributed with C_1, C_2, and C_3.

IV. Conclusion

For the first time, the parameters of a distributed FET model were directly extracted without using optimization techniques. In addition to efficient computation and unique and accurate solution, this method proved the accuracy of our equivalent circuit in modeling the FET's distributive nature.

References

[1] B. Mallet-Guy, Z. Ouarch, M. Prigent, R. Quéré, and J. Obregon, "A distributed, measurements based, nonlinear model of FET's for high frequencies applications," in *IEEE MTT-S Symp.*, Denver, CO, 1997, pp. 869–872.

[2] R. Anholt, *Electrical and thermal characterization of MESFET's, HEMT's and HBT's*. Norwood, MA: Artech House.

[3] J. Portilla, R. Quéré, and J. Obregon, "An improved CAD oriented FET model for large-signal and noise applications," in *IEEE MTT-S Symp.*, San Diego, CA, 1994, pp. 849–852.

[4] G. Ghione, C. Naldi, and F. Filicori, "Physical modeling of GaAs MESFET's in an integrated CAD environnement: From device technology to microwave circuit performance," *IEEE Trans. Microwave Theory Tech.*, vol. 37, pp. 457–468, Mar. 1989.

[5] D.-H. Huang and H. C. Lin, "DC and transmission line models for a high electron mobility transistor," *IEEE Trans. Microwave Theory Tech.*, vol. 37, pp. 1361–1370, Sept. 1989.

[6] J. P. Teyssier, J. P. Viaud, J. J. Raoux, and R. Quéré, "Fully integrated nonlinear modeling and characterization system of microwave transistors with on-wafer pulsed measurements," in *IEEE MTT-S Symp.*, Orlando, FL, 1995, pp. 1033–1036.